Characterization of the Passivation Layer on Disordered Carbons in Lithium-Ion Cells

Ronald Guidotti and Bryan Johnson

Sandia National Laboratories, P.O. Box 5800, Albuquerque, NM 87185-0614

ABSTRACT

Intercalation anodes of graphite or disordered carbon in rechargeable Li-ion batteries (based on aprotic organic solvents) develop a passivating film during the first intercalation of Li^+. The formation of this film reduces the cycling efficiency and results in excessive consumption of Li^+. The exact nature of this film is not well defined, although there are many similarities in properties to the films that form on Li anodes under similar cycling conditions. In this study we report on characterization studies of films formed during galvanostatic cycling of disordered carbons derived from polymethylacryolnitrile (PMAN) in a 1M $LiPF_6$ solution in ethylene carbonate/dimethyl carbonate solution (1:1 by vol.). Complementary tests were also conducted with glass carbon, where intercalation cannot occur. Complex-impedance spectroscopy was the primary measurement technique, supplemented by cyclic voltammetry. The passivation process was associated with two irreversible reduction peaks at ~0.75 V and ~1.1 V vs. Li/Li^+ in the dC/dV-V plot of the galvanostatic data. Similar peaks were displayed in cyclic voltammograms of glassy carbon, but shifted to lower potentials. The PMAN impedance spectra showed inductive behavior during the first intercalation at potentials below 0.5 V. This inductive behavior was related to formation of non-equilibrium reactive intermediates associated with solvent reduction. It was not observed after several intercalation/deintercalation cycles at these potentials. Instead, the impedance spectra exhibited two semicircles and a Warburg-type tail.

Introduction

Lithium ambient-temperature cells use an organic electrolyte as the solvent and a number of Li salts to provide ionic conductivity for Li^+ during charge and discharge. During the cycling of such cells, the Li anode eventually forms dendrites that can cause shorting *(1-2)*. The poor cycling capability of metallic Li under these conditions has spurred interest in the development of alternative anodes that intercalate Li^+.

With an intercalation cell, the Li^+ is shuttled between the anode and cathode during discharge and charge of the cell. This mechanism eliminates the formation of metal dendrites that are associated with Li anodes under the same conditions. This, coupled with the potential for long cycle life, makes the Li-ion-carbon technology very attractive for commercial applications.

The primary material of interest for this application has been partially graphitized (disordered) carbons or graphites. During charging, the Li^+ is desolvated and inserted between the basal planes of the graphite structure. Deintercalation occurs during the reverse (discharge) process.[1] Care must be taken when using polypropylene carbonate (PC) as a solvent, as reaction with PC results in exfoliation of the graphite, which greatly degrades performance

Graphite can form a number of staged compounds with Li *(3)*. The maximum Li content that is normally attained for an ideal graphite structure is LiC_6. This composition is equivalent to charging to a level of 372 mAh/g of carbon. With disordered carbons, however, much higher values have been reported for the first intercalation–in excess of 800 mAh/g, in some instances *(2)*. On deintercalation, however, a much smaller capacity is observed. The difference in the two values is referred to as the irreversible capacity, Q_{irr}, and can be quite large at times–over 400 mAh/g. In some cases, Q_{irr} can be greater than the reversible capacity, Q_{rev} *(2)*.

It is believed that the irreversible capacity results from the formation of a passivation layer on the carbon surface during the first intercalation. This layer is thought to be very similar to the solid-electrolyte-interface (SEI) layer that forms on metallic Li anodes in contact

[1] The actual electronic configuration of the Li during the intercalation process has not been clearly defined; i.e., the extent of ionization or electron delocalization is unkown. For the purpose of this paper, however, we will refer to Li^+ as the intercalation species.

with aprotic organic solutions of Li salts *(4,5)*. It is desirable to minimize Q_{irr}, since extensive passivation results in excessive consumption of Li during the first intercalation.

The passivation layer on carbon or graphite electrodes results from parallel electrochemical processes that involve solvent reduction that takes place at potentials below 0.5 V vs Li/Li^+.[2] The nature of the film is dependent on the type of carbon, the composition of the solvent and supporting electrolyte, and the current density.

A number of techniques have been be used to study the SEI layer on Li. These include x-ray diffraction, Fourier transform infrared spectroscopy (FTIR), x-ray photoelectron spectroscopy (XPS), secondary ion mass spectroscopy (SIMS), Raman spectroscopy, and electrochemical techniques such as cyclic voltammetry and complex impedance *(5)*. In this paper, we report on the use of complex impedance to study the passivation process on disordered carbons derived from polymethylacrylonitrile (PMAN) precursors. Parallel tests were conducted using cyclic voltammetry. Glassy carbon electrodes were also included in the study, as they allowed data to be obtained on a carbon with a well-defined surface area where intercalation was not possible.

Experimental

Materials - The PMAN carbons used in the study were prepared by an inverse emulsion technique, using divinylbenzene (DVB) as a crosslinking agent *(6,7)*. Carbons were pyrolyzed at temperatures of 700°C to 1,100°C under an atmosphere of Ar or Ar/5% H_2. The corresponding BET surface areas ranged from under 10 to over 230 m^2/g.

The solution used for the characterization tests was 1M $LiPF_6$ in ethylene carbonate (EC)/dimethyl carbonate (DMC), in a 1:1 volume ratio. The $LiPF_6$ was obtained from Hashimoto Chemical Corp. and was used as received. The EC and DMC were from Mitsubishi Chemical Co. and were used as received. The water content of the solution, as measured by Karl-Fischer titration, was typically <60 ppm. Li foil (Foote Mineral) was used for the counter and reference electrodes.

Cells - A three-electrode system was used to test all the carbons. The PMAN powder was mixed with 15% polyvinylidene fluoride (PVDF) as a binder and 5% Super 'S' carbon as a conductive additive. The carbon anodes were pasted onto a Cu substrate by the doctor-blade technique using dimethylformamide as the medium. After vacuum drying to remove solvent, anode discs 1.27 cm in diameter (1.27 cm^2 area) were punched from the Cu sheet. Typical thicknesses of the active anode ranged from 0.20 mm to 0.23 mm and the mass of active carbon ranged from 5 mg to 10 mg.

Two 0.25-mm-thick Celgard 2500 separators were used between the working electrode and the counter electrode. The latter consisted of a 0.25-mm thick foil of Li cold-pressed onto a stainless-steel disc. The reference electrode consisted of a Li flag (8-10 mm wide x 0.25 mm thick) perpendicular to the outside edge of the cell, separated by a distance of 2-4 mm. The electrode assembly was loaded into a polypropylene cell and then placed in a secondary container with desiccant.

The cells with the glassy carbon rods used polytetrafluoroethylene (PTFE) feedthrough insulators, so that only the end of the rod was exposed to the solution. The area of the glassy-carbon electrode was 0.07 cm^2.

Cell assembly was conducted in a dry room maintained at a dew point of less than -50°C. The cells were evacuated and backfilled with electrolyte solution in a glove box where the moisture and oxygen content were <10 ppm each. After filling, the cells were allowed to stand overnight before testing.

Apparatus - Galvanostatic testing of the cells was performed using an Arbin Corp. Battery Test System. The test profile consisted of galvanostatic cycling at 0.50 mA/cm^2 between 2 V and 0.01 V for 20 cycles. An open-circuit wait of 600 s was imposed between charge and discharge. The nominal open-circuit voltage (OCV) of a fresh cell was ~3.25 V.

Cyclic voltammograms were generated using a Princeton Applied Research Model 263 potentiostat. The cell was scanned between voltage limits of 3 V and 0.01 V at a sweep rate of 1 mV/s.

Complex-impedance measurements were performed using a Schlumberger Solatron Model 1250 Frequency Response Analyzer coupled to a Solatron Model 1286 Electrochemical Interface. The impedance spectra were normally taken over a frequency range of 65 kHz to 0.10 Hz.

Complex-impedance spectra of the carbon samples during galvanostatic cycling were taken at open circuit before intercalation and under OCV conditions at 2 V, 0.5 V, and 0.01 V during the first intercalation. (Initially, spectra were taken at 0.5 V increments from the starting OCV, but it was subsequently found that these additional measurements were not necessary.) Similar measurements were taken at 2 V, at the end of one complete intercalation/deintercalation cycle. Periodically, complex-impedance measurements were made during subsequent cycles.

Generally, the complex-impedance spectra were performed under OCV conditions–i.e., with no potential applied to the cell–after waiting 300 s after removal of the cell from the galvanostat. During this time, it was noted that the cell potential under OCV conditions did not

[2] All potentials in this report are referenced to Li/Li^+.

always remain stable and increased with time for the intercalation part of the cycle. Subsequent tests also employed a potential-hold technique during complex-impedance measurements, to prevent drifting of the cell potential during these measurements.

Results

PMAN Carbon

Galvanostatic Tests - The electrochemical response of a typical 700°C PMAN carbon during galvanostatic cycling is shown in Figure 1a for the first and second cycles. The curves for the corresponding derivatives of the capacity with respect to voltage vs. the voltage (dC/dV vs. V) are shown in Figure 1b. (Presentation of the data in this form provides information similar to that of a cyclic voltammogram.)

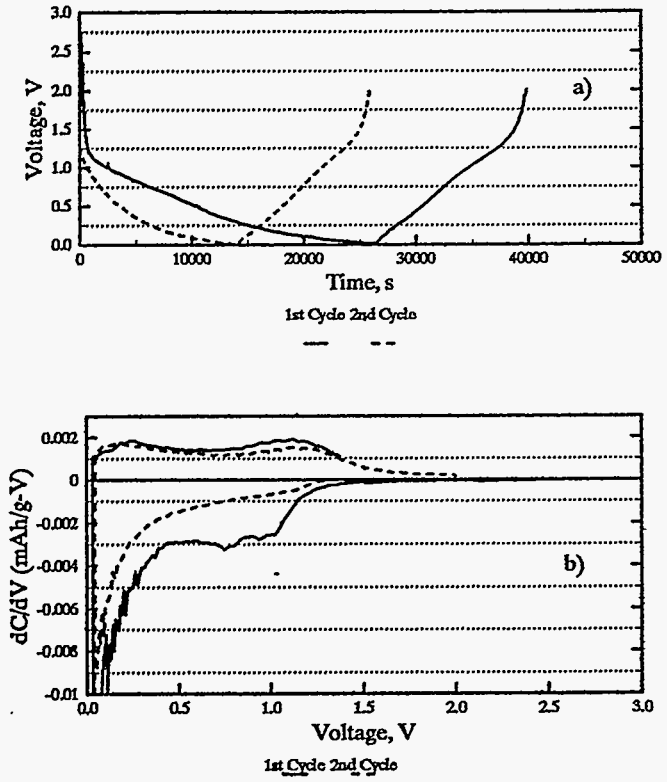

Figure 1. a) First and second galvanostatic cycles of a 700°C PMAN carbon cycled between voltage limits of 2 V and 0.01 V. b) dC/dV vs. V for the same sample.

During the first cycle, the irreversible capacity was found to be comparable to the reversible capacity, or about 400 mAh/g; i.e., the efficiency was only 50%. (With a 1,100°C PMAN, both Q_{irr} and Q_{rev} were reduced but low efficiencies were still obtained.) The bulk of passive-film formation took place during the first cycle. The passivation during the second cycle was only 57 mAh/g for an efficiency of 86%. By the eighth cycle, the efficiency increased to over 97% and remained between 97.6% and 98.8% for the duration of the 20-cycle test.

Two nonreversible reduction peaks are evident in the derivative curves (Fig. 1b), at ~0.75 V and ~1.1 V. These are associated with the formation of the passivation layer, since they were not evident on subsequent cycles.[3] The broad oxidation peak at 1.2 V is not associated with these reduction peaks, as it remains on further cycling. The jagged response below 0.5 V on the first cycle was typical and is associated with noise in the galvanostatic data.

To try to understand the nature of this film, complex-impedance measurements were performed.

Complex Impedance - The complex-impedance spectra of a PMAN carbon prepared at 700°C are shown in Figure 2 under OCV and potential-hold conditions as a

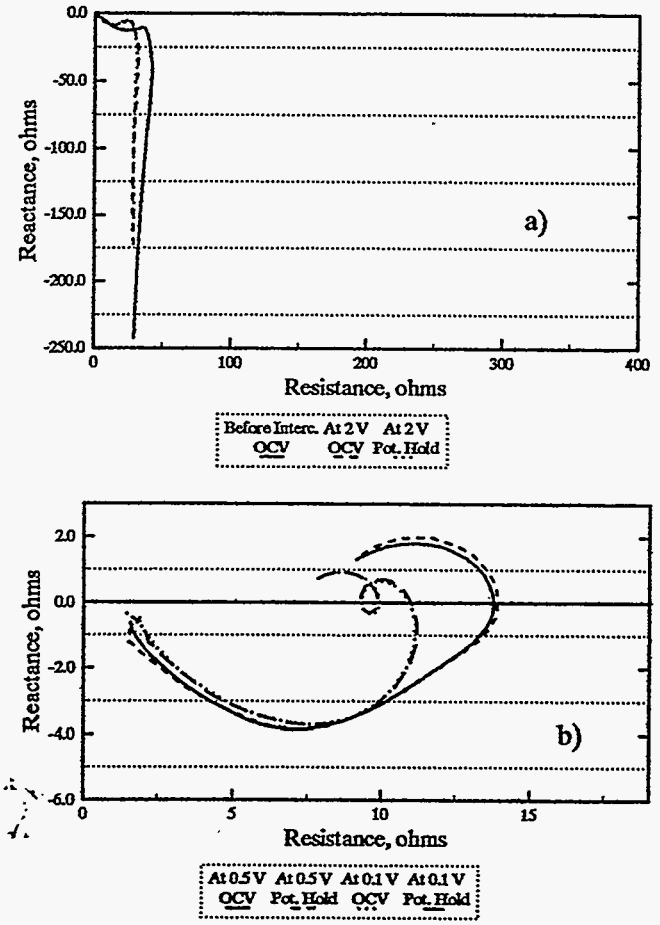

Figure 2. Complex-impedance spectra of 700°C PMAN carbon as a function of potential during the first intercalation. a) Before intercalation and at 2 V; b) at 0.5 V and 0.01 V.

[3] It should be noted that these peaks, observed under constant-current conditions, will *not* be the same as those observed under cyclic voltammetry conditions, where the current is varying dynamically with potential.

function of applied potential during the first intercalation cycle. As expected, the spectrum before intercalation showed capacitive behavior with a large semicircle and a 90° tail characteristic of a porous electrode (Fig. 2a). The spectra at 2 V appeared similar to that prior to intercalation, except that semicircle associated with the charge-transfer process became better defined and smaller in diameter. Identical impedance spectra were obtained under both OCV and potential-hold conditions. This indicates that the reduction processes were essentially at quasi-equilibrium conditions when the cell was removed from the galvanostat at this potential.

The response at potentials below 0.5 V, however, were somewhat surprising, in that a well-defined inductive arc appeared. A similar inductive arc with a loop was observed at the lowest applied potential of 0.01 V (Fig. 2b) (Similar inductive behavior was observed with the PMAN pyrolyzed at 1,100°C.) As can be seen, the spectra were essentially the same under OCV and potential-hold conditions, indicating good electrode stability under these quasi-equilibrium conditions.

The complex-impedance measurements were repeated during subsequent intercalation cycles, to observe the effect on the spectra. While the bulk of the passive film formation occurs during the first intercalation, some additional formation occurs at a low rate during subsequent cycles. The impedance behavior of the electrode would be expected to reflect these changes in morphology and structure.

The complex-impedance spectra for the 700°C PMAN carbon at 2 V after one complete intercalation/deintercalation cycle showed a semicircle and Warburg tail. The inductive component was still evident at 0.5 V and 0.01 V on the second and third cycles, however, but at a much reduced level. This indicates some passive-film formation was still occurring under these conditions.

The complex-impedance spectra after 16 complete cycles are shown in Figure 3 for this same material. The spectrum at 2 V showed a semicircle and a Warburg-like tail (Fig. 3a). (The high-frequency part of the curve is expanded in the insert in Fig. 3a for the resistance region 0 to 40 ohms.) These are associated with charge transfer during film formation (solvent reduction) and diffusion of Li^+ through the passive film.

The spectra at 0.5 V and 0.01 V (Fig. 3b) showed two semicircles and a Warburg-type tail. The tail for the 0.5 V data was not very evident at the low-frequency limit of 0.10 Hz. It became well defined for the 0.01 V data, however, when the frequency was reduced to 0.3 mHz. The low-frequency semicircle is most likely associated with the intercalation processes involving Li^+.

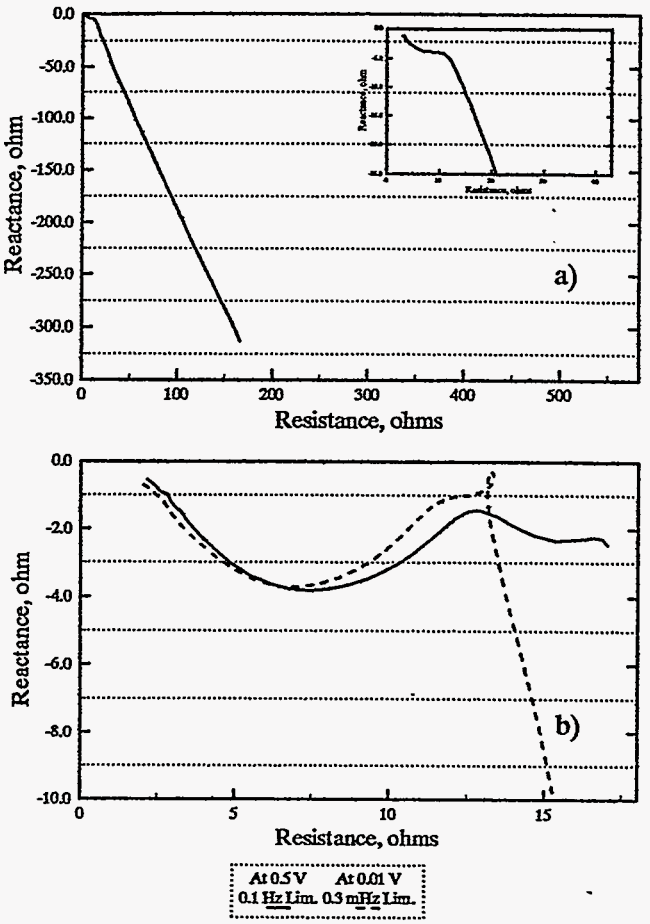

Figure 3. Complex-impedance spectra of 700°C PMAN carbon as a function of potential during the 17th intercalation cycle. a) At 2 V; b) at 0.5 V and 0.01 V.

Glassy Carbon

Cyclic Voltammetry - Cyclic voltammetry (CV) experiments were run on the glassy carbon, in an attempt to better define the electrochemical processes associated with formation of the passive film during cycling of PMAN carbons. Since the glassy carbon lacks the graphene sheets associated with disordered carbons and graphites, no intercalation of Li^+ is possible. Thus, the predominant electrode process during reduction should be passive-film formation. The results of the CV tests are summarized in Figure 4 for the first three scans.

Three irreversible reduction peaks associated with the formation of the passive film were observed during the first cycle: two broad peaks (shoulders) at 1.7 V and 1.2 V and a major peak at 0.45 V. The latter two are consistent with the derivative data of Fig. 1b, but are shifted in potential (see Footnote 2). The peak at 1.7 V may be due to an electroactive impurity in the solution.

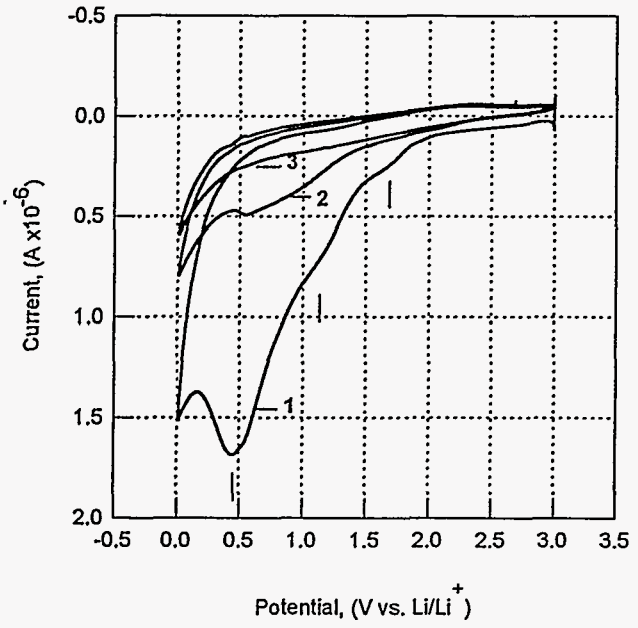

Figure 4. Cyclic voltammograms for glassy carbon for three cycles. Scanned from 3 V to 0.01 V at 1 mV/s.

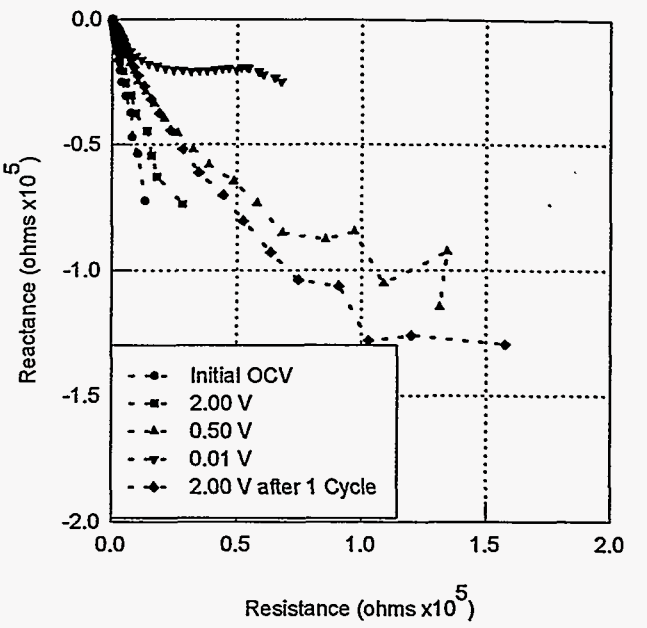

Figure 5. Complex-impedance spectra of glassy carbon at OCV as a function of applied potential during first reduction.

The broad shoulders disappeared on the second scan and the peak at 0.45 V was substantially reduced, indicating reduced film formation. By the third cycle, very little film formation was occurring. The irreversibility was readily evident in the current efficiencies for the three cycles. The efficiency for the first cycle was only 18.7% which increased to 24.5% and 26% for the second and third cycles, respectively.

These data suggest that passive-film formation proceeds slowly over multiple cycles on a planar glassy-carbon surface where the surface area is very small. In comparison, film formation for the PMAN carbons. which have a relatively high surface area, is essentially complete during the first reduction.

The reduction peaks we observed with glassy carbon with our electrolyte are similar to what has been reported by Inaba *et al.*, for CVs of highly oriented pyrolytic graphite (HPOG) in 1M $LiClO_4$/EC-diethyl carbonate (DEC) solution *(8)*. They observed a major peak at 0.733 V, with two smaller ones are 0.558 V and 0.427 V. These were associated with reduction of the EC-DEC solution and were irreversible. The reduction process was initiated near 1.1 V for their electrolyte system. These data are consistent with our observations with glassy carbon in our electrolyte.

Complex Impedance - The complex-impedance spectra of the glassy carbon at OCV (no potential hold) are shown in Figure 5 as a function of potential during the first reduction cycle under galvanostatic conditions. (The same results were obtained when these tests were repeated under potential-hold conditions.) The lower frequency limit for these tests was increased to 1 Hz from 0.1 Hz because of the large scatter in the data at low frequencies.

The response at OCV before passage of current was that of a simple capacitor in series with a solution resistance of ~4.5 ohms. The capacitance calculated from the low-frequency limit was 2.8 μF *(9)*. This compares to a capacitance of 4,700 μF for the 700°C PMAN calculated in the same manner. A similar electrode response was observed at 2 V.

However, when the potential was reduced to 0.5 V, where passivation would be expected to be extensive, no inductive arc or loop occurred as for the PMAN carbon under the same conditions (Figure 2b). The spectrum at 0.01 V showed mostly a charge-transfer process coupled with a possible Warburg-type diffusion. The spectrum at 2 V, after one complete cycle, looked very similar to that for 0.5 V during reduction; the surface no longer appeared as a simple capacitor as it did with no passage of current.

The complex-impedance spectra for the second cycle did not differ markedly from those of the first cycle, indicating that the electrode processes during repeated cycling were similar and involved the formation of the passive film.

As shown in Figure 6, the cell potential was not stable when the cell was gated to open circuit before stepping to lower potentials (i.e., 2 V , 0.5 V, and 0.01 V) during the galvanostatic tests. The potential increased rapidly on open circuit, indicating that the cell was not at

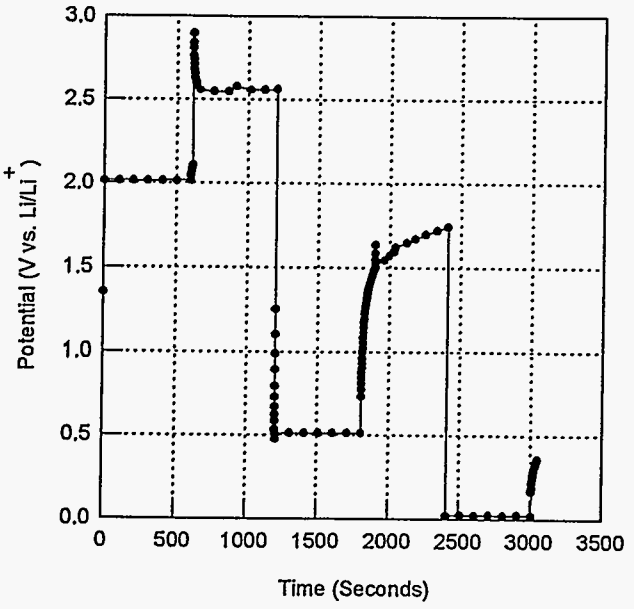

Figure 6. Cell potential of glassy-carbon electrode during galvanostatic cycling tests where complex-impedance measurements were taken at OCV as a function of applied potential during first reduction.

equilibrium. The rate of increase of the open-circuit potential of the glassy carbon between voltage steps was considerably less with subsequent cycles, indicating the electrode was moving closer to equilibrium with repeated cycling.

The same voltage instability was exhibited by PMAN carbons when they were removed from the potentiostat and placed immediately under OCV condition prior to impedance measurements. It was not as pronounced, however, as for glassy carbon. The rate of increase was significantly reduced if the cells were held at a fixed potential and the current allowed to decay to a low value (typically <20 μA) prior to removal from the galvanostat.

The formation of the passive film on the glassy carbon under these conditions was more controlled and limited relative to the PMAN carbon. The glassy-carbon electrode had a much lower surface area than the PMAN electrode–0.07 cm^2 vs. 1480 cm^2, respectively. Li^+ is prevented from intercalating into the glassy carbon because it lacks the lamellar structure of the disordered carbons and graphite. Thus, the behavior of the glassy carbon under galvanostatic cycling reflects the formation of the passive film from solvent decomposition (from chemical and electrochemical processes) without the complications of intercalation reactions.

Discussion

Similar inductive behavior in the impedance spectra for PMAN carbons in this work has been noted for the electrodeposition of Ni from H_2SO_4 solutions *(10-13)*. In that case, the inductive behavior was attributed to reactive intermediates. In the present work, the inductive behavior is believed to be associated with chemisorption and reduction of reactive intermediates associated with the reduction of solvent on high-surface-area PMAN carbon.

Complex-impedance spectra have been reported for mesophase pitch-based carbon fibers by Takami *et al.* as a function of extent of intercalation *(14)*. They also used 1M $LiPF_6$ in their work but with an EC and PC mixture. Their spectra during the first intercalation showed a distorted semicircle and a weak Warburg-type tail for carbons prepared at 900°C. The diameter of the semicircles for the charge-transfer process decreased as x increased from 0.1 to 0.65 in Li_xC_6 during intercalation. There was no evidence of any inductive component in their spectra.

In recent work, Zaghib *et al.*, measured the complex impedance of a disordered meso-carbon prepared at 700°C *(15)*. Spectra were taken at decreasing potentials from 500 mV to 0 V during intercalation. The carbon-anode response changed considerably as a function of potential. Their data also showed the presence of a small inductive component during the first intercalation. The magnitude of the inductance was much less than what was observed in our work, however. More importantly, the inductive behavior was observed at high frequencies, while we observed it only at low frequencies (<3 Hz). The inductive response for their cell could have been associated with cell leads.

At 500 mV, a semicircle was observed which became smaller in diameter when the potential was reduced to 200 mV, with concomitant development of a Warburg-type tail. At 80 mV and 0 V, additional semicircles appeared at low frequencies. These could be associated with intercalation of Li^+ or electrodeposition of Li. This work indicates that the first intercalation process can be quite complicated in the case of disordered carbons, where multiple reactions involving solvent reduction can occur.

Zaghib *et al.* found that the complex impedance spectra of a carbon graphitized at 3,000°C exhibited a simple charge-transfer processes (well-defined semicircle) coupled with a diffusion process (Warburg tail) *(15)*. The diameter of the semicircle decreased with as the applied potential during intercalation was reduced from 500 mV to 0 V, much as for the 700°C carbon. However, there was no evidence for any induction processes for the high-temperature carbon. In addition, there was an absence of multiple semicircles at potentials below 80 mV which contrasts markedly with the data for the 700°C carbon.

The data by Zaghib *et al.* indicate that the extent of order in the carbon has a strong impact upon the nature of the passive film that forms during the initial intercalation of Li^+. This parallels our experience with PMAN carbons,

where both the reversible and irreversible capacity are a strong function of pyrolysis temperature. However, both the high- and low-temperature PMAN carbons exhibited inductive behavior in their impedance at potentials below 0.5 V.

The question arises then as to what is responsible for the inductive behavior we observed during intercalation of PMAN carbons. There are a number of possible explanations. One possibility is the inductive behavior resulted from the cell and test configuration used. This was not observed, however, with graphitic or well-ordered samples; the behavior was material specific. This eliminates the possibility that the inductive response was an artifact of the test cell.

A second possibility is the inductive behavior involved plating of elemental Li onto the carbon surface or in the pores during intercalation. This might be a possibility for the complex-impedance measurements made at the lowest intercalation potential of 0.01 V, if the galvanostat were not calibrated properly. This possibility can also be dismissed, since the inductive response disappears after the cell is cycled several times; it is only observed on the *initial* intercalation. The possibility of undervoltage deposition of Li at the lower potentials can similarly be discounted.

The lack of Li plating is also reflected in the shape of the complex-impedance spectra. Only a semicircle associated with charge transfer was reported for the impedance spectra for Li in tetrahydrofuran (THF) solutions; no Warburg behavior was observed *(16)*. Preliminary complex-impedance measurement in our laboratory of Li with our electrolyte system corroborates these results.

The most reasonable explanation of the inductive behavior involves the formation of reactive molecular species on the carbon as a result of reduction of solvent during initial intercalation. The reduction steps very likely involve chemisorption processes as well. The high surface area of the carbon (32 m^2/g) would be expected to enhance the reduction of solvent under these conditions. This is consistent with the formation of complex species observed during Ni electrodeposition *(13)*.

The following discharge mechanism and processes are proposed to explain the observed complex-impedance of PMAN carbons in 1M $LiPF_6$/EC-DMC solutions.

At OCV, before intercalation, the electrode displays predominantly capacitive behavior, due to the double layer. At 2 V during the *first* intercalation, charge transfer and diffusion processes associated with initiation of the formation of the passive film are indicated. The size of the semicircle suggests that these processes are not very facile at this potential. At 0.5 V, however, the Warburg-type response disappears and significant inductive behavior is observed. This is associated with the reduction of solvent during active formation of the passive film which begins near 1.1 V and is enhanced at 0.75 V. The intercalation of Li^+ under these conditions is limited. At 0.01 V, film growth continues, along with increased intercalation of Li^+. These processes are occurring in parallel and are not resolved in the complex-impedance spectra.

After deintercalation to 2 V, the carbon is covered with a passive film. Intercalation during subsequent cycling then requires diffusion of Li^+ through this film to complete the charge-transfer process. This gives rise to the semicircle and Warburg-type tail in the impedance spectrum, much like that for spectrum at 2 V during the first intercalation (Fig. 2a).

Intercalation during the *second* cycle results in additional formation of the passive film, but at a much reduced level compared to the first cycle. Consequently, some inductive behavior is still observed in the impedance spectra at 0.5 V and 0.01 V. After three or four cycles, a cohesive electrochemically stable passive film has been established. When reducing potentials below 0.5 V are subsequently applied to the carbon, the intercalation of Li^+ becomes the predominant electrode process. This is manifested in the impedance spectra by a low-frequency second semicircle which has a diameter much smaller than the high-frequency semicircle associated with passive-film formation. The diameter of the low-frequency semicircle decreases at more reducing (lower) potentials, due to enhanced kinetics.

Future tests with SIMS and XPS are planned to obtain information on the chemical nature of the passive film, including speciation.

Conclusions

A passive film forms during galvanostatic cycling of PMAN carbons over a potential range of 2 V to 0.01 V. The bulk of the film formation occurs irreversibly during the first reduction step at potentials of between ~1.1 V and ~0.75 V vs Li/Li^+; corresponding anodic peaks are not observed. These reduction peaks are not observed on subsequent cycles. With a 700°C PMAN carbon, the formation of the passive film corresponds to half of the total capacity of the first intercalation step of 800 mAh/g. On subsequent cycles, passive-film formation is minimal. Similar behavior is exhibited by the 1,100°C PMAN, except that the total capacity during the first cycle is only about half of that for the 700°C PMAN

The complex-impedance spectra of PMAN carbons are very voltage dependent. Generally, capacitive behavior is shown before intercalation. At 2 V during the first intercalation, a weak semicircle and Warburg tail appear. These are associated with charge-transfer and diffusion of Li^+ across the passive film that begins to

form at this potential during the first reduction step. Below 0.5 V, a significant inductive arc or loop appears in the impedance spectra during the first intercalation. It is proposed that this behavior is associated with the formation of reactive surface groups on the high-surface-area carbon under dynamic, non-equilibrium conditions. These intermediates result from the reduction of solvent and exist predominately during the first intercalation. They are still present to a limited extent during the second and third intercalation cycles. After several cycles, however, two semicircles and a Warburg tail are formed. The high-frequency semicircle and Warburg tail are associated with the passive which has now become well established. The much smaller low-frequency semicircle is associated with the more facile Li^+-intercalation process. The impedance spectra at 2 V after complete deintercalation show only a well-defined semicircle and Warburg tail.

Cyclic voltammetry and complex-impedance measurements glass-carbon electrodes allowed characterization of the passivation layer without the complications of Li^+ intercalation. Film formation proceeds readily and irreversibly on the first cycle. Further film growth is dramatically slowed on subsequent cycles. The complex impedance spectra for the passivation process show a semicircle and pseudo-Warburg tail. The reduction peaks associated with passive-film formation are shifted slightly to more-positive potentials for the glassy carbon compared to PMAN. The data for the glassy carbon corroborate the mechanism proposed for passive-film formation on disordered PMAN carbons.

Acknowledgments

The authors are grateful to W. R. Even. Jr., Sandia National Laboratories, Livermore, CA, for providing the PMAN carbon samples. Mariette Reber prepared the electrodes and assembled the cells, and Leo Griego and Herb Case tested the cells. Frank M. Delnick provided insightful suggestions regarding the complex-impedance data.

This work was supported by the United States Department of Energy under Contract DE-AC04-94AL85000.

REFERENCES

1. Dahn, J. R., Sleigh, A. K., Shi, H., Way, B. M., Weydanz, W. J., Reimers, J. N., Zhong, Q., and von Sacken, U., "Carbons and Graphites as Substitutes for the Lithium Anode," in *Lithium Batteries,* Pistoia, G., Ed.:Elsevier, New York, 1994; pp. 1-48.
2. Zheng, T., Liu, Y., Fuller, E. W., Tseng, S., von Sacken,U., and Dahn, J. R., *J. Electrochem. Soc.*, **1995**, *142* (8), 2581.
3. Guerard, D. and Herold, A., *Carbon*, **1975**, *13*, 337.
4. Aurbach, D., Ein-Ely, Y., and Zaban, A., *J. Electrochem. Soc.*, **1994**, *141* (1), L1.
5. Aurbach, D., Daroux, M. L., Faguy, P. W., and Yeager, E., *J. Electrochem. Soc.*, **1988**, *135* (8), 1863.
6. Even, W. R. and Gregory, D. P., *MRS Bulletin*, **1994**, *XIX* (4), 29.
7. Delnick, F. M., Even, Jr., W. R., Sylwester, A. P., Wang, J. C. F., and Zifer, T., **U.S. Patent 5,426,006**, June 20, 1995.
8. Inaba, M., Siroma, Z., Zempachi, O., Takeshi, A., Mizutani, Y., and Asano, M., *Chem. Letters*, **1995**, 661.
9. Delnick., F. M., Jaeger, C. D., and Levy, S. C., *Chem. Eng. Commun.* **1985**, *35*, 23.
10. Epelboin, I, and Keddam, M., *Electrochim. Acta*, **1972**, *17*, 177.
11. Feller, H. G., Ratzer-Scheibe, H. J., and Wendt, W., *Electrochim. Acta*, **1972**, *17*, 187.
12. Epelboin, I, Jousselin, M, and Wiart, R., *J. Electroanal. Chem.*, **1979**, *101*, 281.
13. Epelboin, I, and Wiart, R., *J. Electrochem. Soc.*, **1971**, *118*, 1577.
14. Takami, N., Satoh, A., Hara, M., and Ohsaki, T., *J. Electrochem. Soc.*, **1995**, *142* (2), 371.
15. Zaghib, K. Tatsumi, K., Imamura, T., Sawada, Y., and Higuchi, S., "Electrochemical Intercalation of Lithium in Different Origin of Carbon Materials as Negative Electrodes for Lithium Ion Rechargeable Batteries," *187 Meeting of the Electrochemical Society*, Reno, NV, May 21-26, 1995.
16. Aurbach, D., Zaban, A., Gofer, Y., Abramson, O., and Ben-Zion, M., *J. Electrochem. Soc.*, **1995**, *142* (3), 687.